

THE NUCLEAR COLORS AND MORPHOLOGY OF FIELD GALAXIES AT MODERATE REDSHIFT¹

DUNCAN A. FORBES, REBECCA A. W. ELSON,² ANDREW C. PHILLIPS,
 GARTH D. ILLINGWORTH, AND DAVID C. KOO

Lick Observatory, University of California, Santa Cruz, CA 95064

Received 1994 August 5; accepted 1994 October 3

ABSTRACT

Until recently, the study of faint field galaxies has been limited by the spatial resolutions available to ground-based imaging. Here we present *HST* images with 0".1 resolution for a sample of 203 field galaxies with $I \leq 22$ (corresponding to $B \leq 24.5$). The expected median redshift for such a sample is $z \sim 0.5$. The high resolution of *HST* allows us to measure the nuclear (central-kiloparsec) color. We have also classified the morphological type of each galaxy and noted any signs of peculiarities or the presence of nearby galaxies. For the brightest third of the sample, familiar Hubble types have been assigned. Combining the types with nuclear colors, we find weak evidence that merging/interacting galaxies have bluer colors than noninteracting galaxies.

Subject headings: galaxies: evolution — galaxies: formation — galaxies: structure

1. INTRODUCTION

Galaxy morphology has been known to correlate with environment since the work of Hubble & Humason (1931) over 50 years ago. Spiral galaxies generally inhabit low-density regions such as the field or the outer parts of clusters, while elliptical galaxies are common near cluster centers. Subsequent studies have refined this “morphology-density relation,” showing that there is a fairly continuous distribution of the morphological-type fraction with environmental density (e.g., Dressler 1980; Postman & Geller 1984; but see also Whitmore, Gilmore, & Jones 1993). This relation provides a fundamental clue as to the evolutionary processes affecting galaxies. One extreme view is that the galaxy type is “imprinted” at the formation epoch so that disks are favored in low-density environments and elliptical galaxies in high-density ones. Alternatively, disks could be destroyed by violent collisions which lead to the formation of elliptical galaxies. Morphological studies of cluster and field galaxies with look-back time could help to determine which of these processes dominates.

Field galaxies are interesting in their own right and are currently the subject of considerable debate. For example, the blue galaxies that dominate number counts at faint magnitudes may be fading dwarfs (Babul & Rees 1992) or, alternatively, galaxies undergoing a merger (Broadhurst, Ellis, & Glazebrook 1992). A crucial ingredient missing from most previous studies is detailed structural information. Only a few ground-based studies exist of moderate-redshift galaxies obtained under exceptional seeing conditions (e.g., Lavery, Pierce, & McClure 1992). Significant gains have been made here with the *Hubble Space Telescope* (*HST*) and the first wide field camera (WFC-I), not only because of its superior resolution but also because the “sky” background is much lower (e.g., Phillips et

al. 1994a; Dressler et al. 1994; Couch et al. 1994; Griffiths et al. 1994b). Further major gains are expected for *HST*'s WFC-II with its substantially better image concentration.

Here we present an *I*-band magnitude-limited sample of 203 galaxies from nine early WFC-II images observed as part of the Medium Deep Survey (MDS; see Griffiths et al. 1994b). These images should be representative of galaxies in the field. Several images are in common with those of Griffiths et al. (1994a), who visually classified galaxies according to a basic morphological scheme. Our magnitude limit ($I \leq 22$) indicates a median redshift of $z \sim 0.5$ (Lilly 1993; Tresse et al. 1993), which corresponds to a look-back time of ~ 5 Gyr. At this distance, the resolution of WFC-II allows us to probe structures on scales of a kiloparsec. From these data we visually assign a Hubble type where possible and identify galaxies with signs of an ongoing merger or interaction. Nuclear (central kiloparsec) colors for these galaxies and “normal” galaxies are compared. Future papers discussing other aspects of WFC-II MDS galaxies include Glazebrook et al. (1994) and Phillips et al. (1994b).

2. OBSERVATIONS AND DATA REDUCTION

The data used in this study are summarized in Table 1. These MDS images were taken in “parallel mode” several arcminutes from the primary target, in random locations at high Galactic latitude. They contain only a few Galactic stars. The POSS plates show no evidence for a cluster of galaxies within several arcminutes of our MDS field of view (fov), consistent with the galaxies representing a field population. We selected MDS fields with multiorbit F814W (I_{814}) images; most also have F606W (V_{606}) images. Initial data reduction used the STScI pipeline software, with the following calibration files: dbu1424mu (bias), e1q1433du (dark), dcd1539ku (F814W flat), and dcd1430mu (F606W flat). The current procedure should be accurate to a few percent, which is sufficient for our purposes. Images were aligned and combined using a modified version of the IRAF task NEWIMCOMBINE, kindly supplied by K. Glazebrook. Cosmic rays and hot pixels were effectively removed with a 3σ rejection criterion based on

¹ Based on observations with the NASA/ESA *Hubble Space Telescope* obtained at the Space Telescope Science Institute, which is operated by AURA, Inc., under NASA contract NAS 5-26555.

² On leave from the Institute of Astronomy, Madingley Road, Cambridge CB3 0HA, UK.

TABLE 1
OBSERVATIONS

MDS Field (1)	Date (2)	l (3)	b (4)	N_V (5)	T_V (6)	N_I (7)	T_I (8)
U001	1994 Jan 26	178.48	-48.11	2	2400	5	6600
U002	1994 Feb 09	233.67	-62.42	2	1500	2	4200
U003	1994 Feb 10	35.78	56.51	2	3300	4	7500
U004	1994 Feb 12	133.95	-64.91	1	1200	2	4200
U005	1994 Feb 12	133.93	-64.93	2	3300	3	6300
U006	1994 Feb 13	123.68	-50.30	5	8700	6	12600
U008	1994 Feb 20	33.87	66.75	6	5200	6	6000
U013	1994 Feb 28	145.54	64.98	2	2000
U014	1994 Mar 03	16.04	39.90	6	5200	6	6000

Col. (1).—MDS field. Col. (2).—Date of observation. Col. (3).—Galactic latitude. Col. (4).—Galactic longitude. Col. (5).—Number of V_{606} exposures. Col. (6).—Total V_{606} exposure time (s). Col. (7).—Number of I_{814} exposure. Col. (8).—Total I_{814} exposure time (s).

the detector characteristics. The scale is $0''.1 \text{ pixel}^{-1}$, giving a fov of $\sim 1.3 \times 1.3$ for each of the three CCDs.

3. PHOTOMETRY AND NUCLEAR COLORS

Our first task in defining a galaxy sample is to identify all galaxies in the fields listed in Table 1, to a limiting magnitude. We used photometric zero points of $I_{814} = 21.67$ and $V_{606} = 22.84$. These are appropriate for data pipeline-processed before 1994 mid-March and should be accurate to within a few percent (Holtzman et al. 1994). Magnitudes were measured using the PHOT task in DAOPHOT. We used circular apertures to construct a curve of growth. From these and visual inspection of each galaxy we determined an appropriate aperture for the total light; in some cases this involved a small extrapolation of the curve of growth. For most galaxies an aperture of 20 pixels ($2''$) radius was used, with the sky determined by the mode in an annulus between 80–90 pixels. The sky annulus was adjusted in special cases where a galaxy was near the edge of the chip or near another bright object. A list was made of all galaxies with $I_{814} \leq 22.0$ and FWHM sizes greater than 2.5 pixels, so any objects such as stars, very compact galaxies, or QSOs are not included in our sample. We also measured a “nuclear magnitude” in a 3 pixel ($0''.3$) radius aperture. Table 2 lists for each galaxy its $V_{606} - I_{814}$ nuclear color and total I_{814} mag. For typical galaxy colors at moderate redshift (Frei & Gunn 1994), Cousins $I \approx I_{814} - 0.1$.

Fields U004 and U005 overlap by half a chip. For the seven galaxies in common, the typical uncertainty in the nuclear color is ± 0.05 mag and for the total I_{814} magnitude, ± 0.1 mag. Thus our internal consistency is of the same order as the absolute photometric uncertainty, i.e., ≤ 0.1 mag. Average magnitudes were adopted for these seven galaxies. The completeness of our sample can be estimated by comparison with I -band galaxy counts in the literature (see Fig. 11 of Phillips et al. 1994a). The effective area for our sample is 0.0113 deg^2 . When scaled by area, our sample is effectively 100% complete to $I \leq 21$ (94 galaxies) and $\sim 70\%$ to $I \leq 22$ (203 galaxies).

Redshifts have not yet been obtained for individual galaxies. The redshift for our sample can, however, be estimated statistically from the field galaxy surveys of Lilly (1993) and Tresse et al. (1993). These studies indicate a median redshift of $z \sim 0.4$ for $I \leq 21$ and $z \sim 0.5$ for $I \leq 22$, with a large range $0.2 < z < 1.0$. Our magnitude limits correspond to $B \leq 23.6$ (for $z = 0.4$) and $B \leq 24.7$ (for $z = 0.5$) for a typical Sbc galaxy (Frei & Gunn 1994).

4. VISUAL MORPHOLOGY

Morphological classification of the galaxies was carried out by visually examining both the I_{814} and V_{606} images. These filters correspond roughly to rest-frame B and V at $z = 0.5$, and so the galaxies can be compared with local examples classified from photographic plates. We used the Hubble Atlas (Sandage 1961) as our template. Our classification is included in Table 2. For the majority of galaxies with $I_{814} < 21$, we are confident that reliable Hubble types could be assigned, i.e., they were similar to local counterparts, although sometimes with signs of peculiarities. At fainter magnitudes we generally chose a less fine classification based on whether the galaxies appeared to be either bulge-dominated, intermediate, or disk-dominated systems. We have about 50 galaxies in common with Phillips et al. (1994b), and comparison of the classification between DAF and ACP gave good agreement, with typical differences of plus or minus one Hubble class or less (e.g., Sa to Sb), with little or no systematic trend. This gives us confidence that our classification is fairly independent of the reviewer. Hubble types are strongly related to a galaxy’s bulge-to-disk ratio, so as a credibility test of our classification we have examined the dependence on the concentration of light, which is a crude measure of bulge-to-disk ratio. Comparing the ratio of nuclear-to-total flux against our Hubble types indicates, as expected, that early-type galaxies have a higher concentration of light than later types, and that our classification has some real physical significance.

In addition to this approach, we noted whether a galaxy showed visual evidence for an ongoing merger/tidal interaction. We have adopted the following criteria: a disturbed morphology and nearby companions (another galaxy of up to ~ 2 mag fainter within ~ 2 diameters of the brighter galaxy), see galaxies 40 and 42, or a system in which two distinct sub-systems are contained within a common envelope (e.g., galaxy 51). We have classified 30% of our sample to be merging/interacting. These classifications can be improved when redshifts become available for each galaxy so that chance projections can be excluded.

5. RESULTS AND DISCUSSION

The 75 brightest galaxies ($I_{814} < 20.8$) in our sample are displayed in Figure 1 (Plates L1–L3). In some cases, classification as a merging/interacting system is not obvious from this Figure, as either the distortion of the isophotes is at low contrast or the interacting galaxy lies beyond the subframe. It is worth commenting on some galaxies individually. The two bluest Ep galaxies (Nos. 11 and 30) both show tidal features at low contrast, toward nearby companions. The reddest Ep (galaxy 21) appears to show some signs of central dust. The elliptical galaxy 46 shows a jetlike feature nearby. Other notable galaxies include No. 13, which is an edge-on dusty spiral with no evidence of a bulge. A ring of star formation surrounding the nucleus is seen in galaxy 29. Galaxies 19 and 20 appear to be highly distorted disks undergoing strong interaction and star formation. At our fainter magnitudes, we see a large number of disk-dominated systems, but we cannot distinguish whether they are distant spirals or intrinsically faint, low surface brightness objects.

If we take ellipticals (Ell) to include types E, i, E/S0, and lenticulars (Len) to include types S0, i, S0/a, and spirals plus irregulars (Sp + Irr) to include Sa–Sd, Irr, we find our sample of 203 galaxies to have a Ell/Len/(Sp + Irr) mix of $\sim 19/19/$

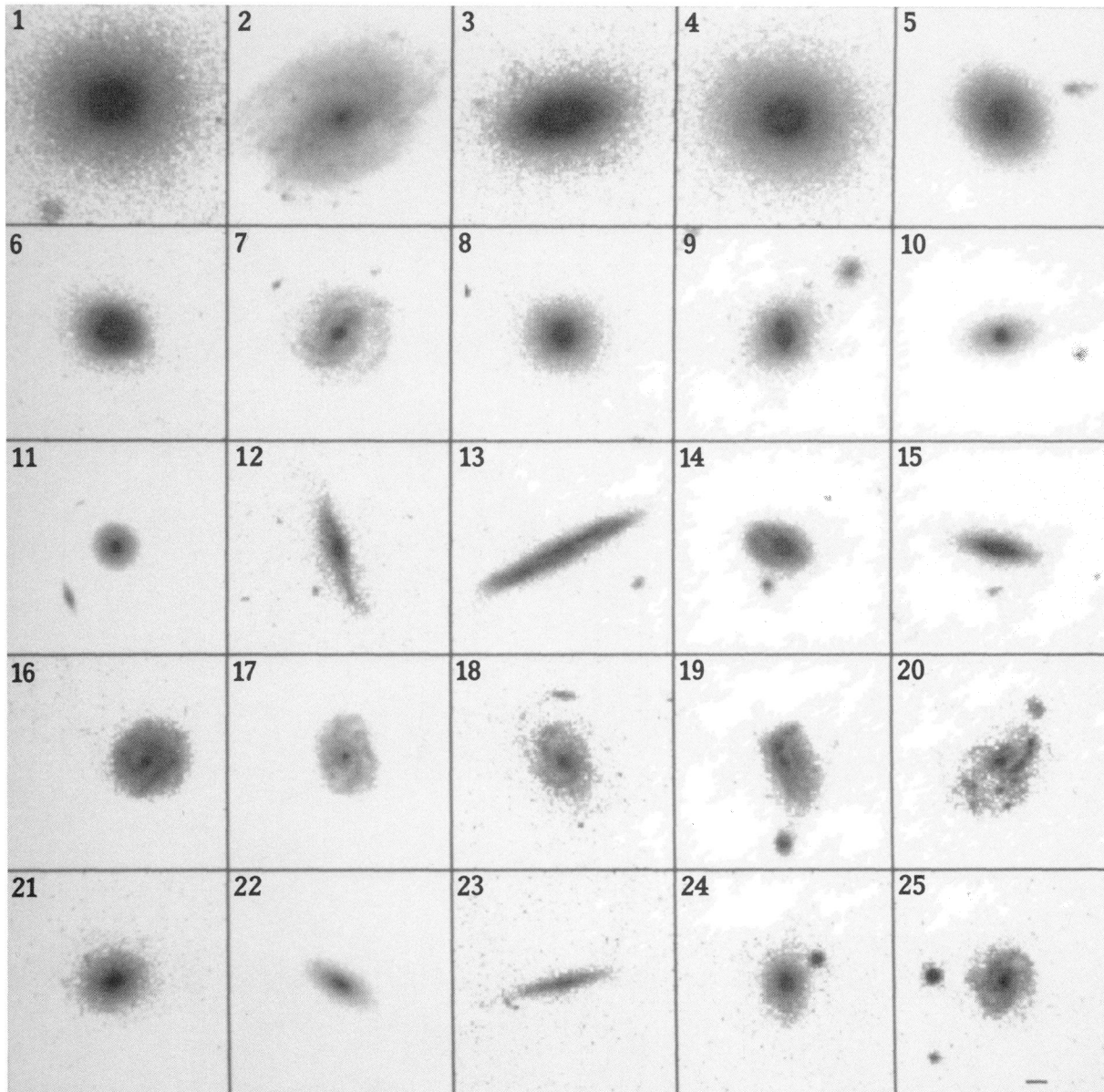


FIG. 1.—Montage of the 75 brightest galaxies ($16.5 < I_{814} < 20.8$) ordered from left to right and from top down. The galaxy of interest lies closest to the center of the subframe. The image display is logarithmic. A $1''$ bar (corresponding to $4 h^{-1}$ kpc at $z = 0.5$, $q_0 = 0.05$) is shown in the lower right subframe.

FORBES et al. (see 437, L18)

PLATE L2

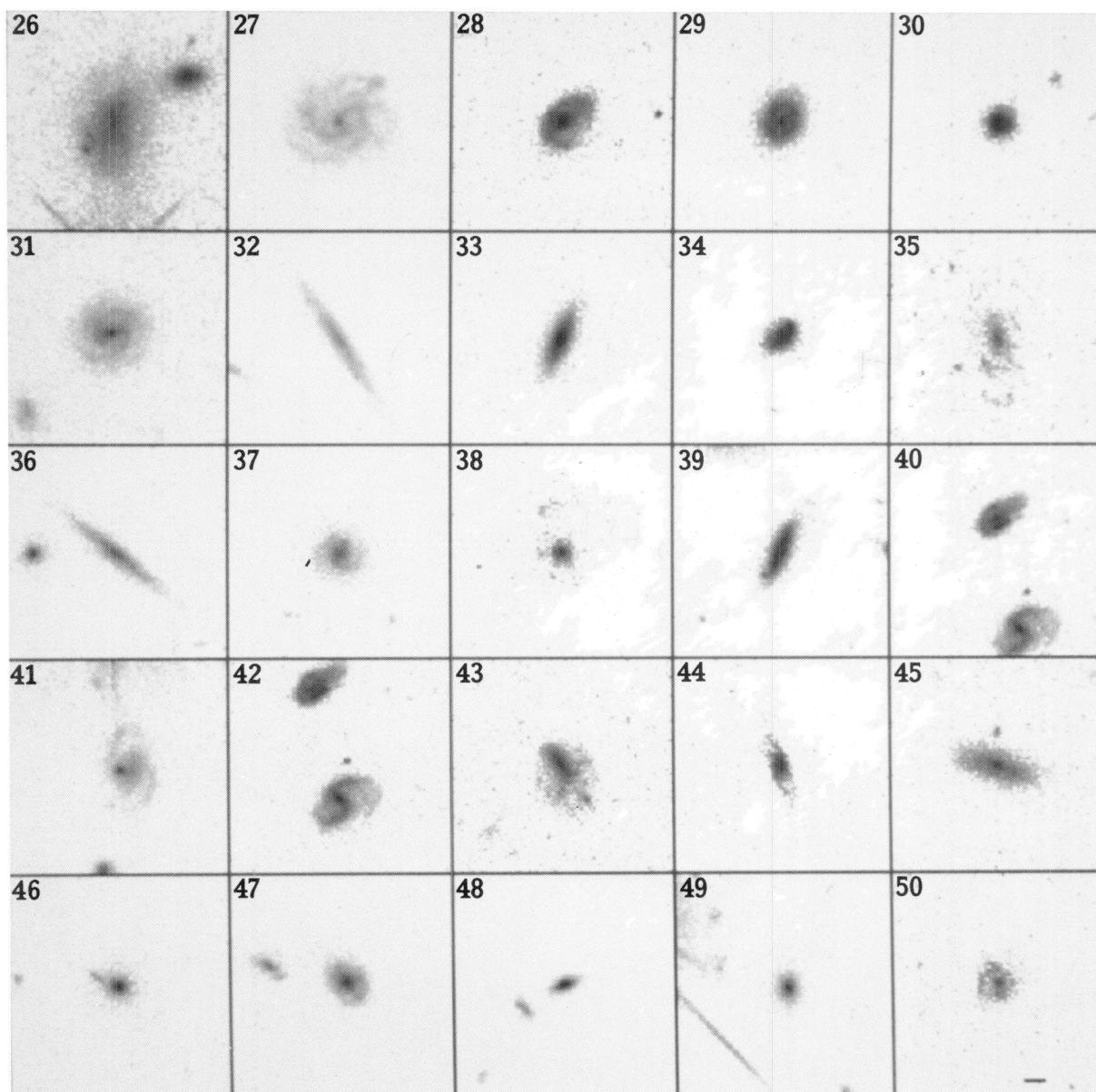


FIG. 1—Continued

FORBES et al. (see 437, L18)

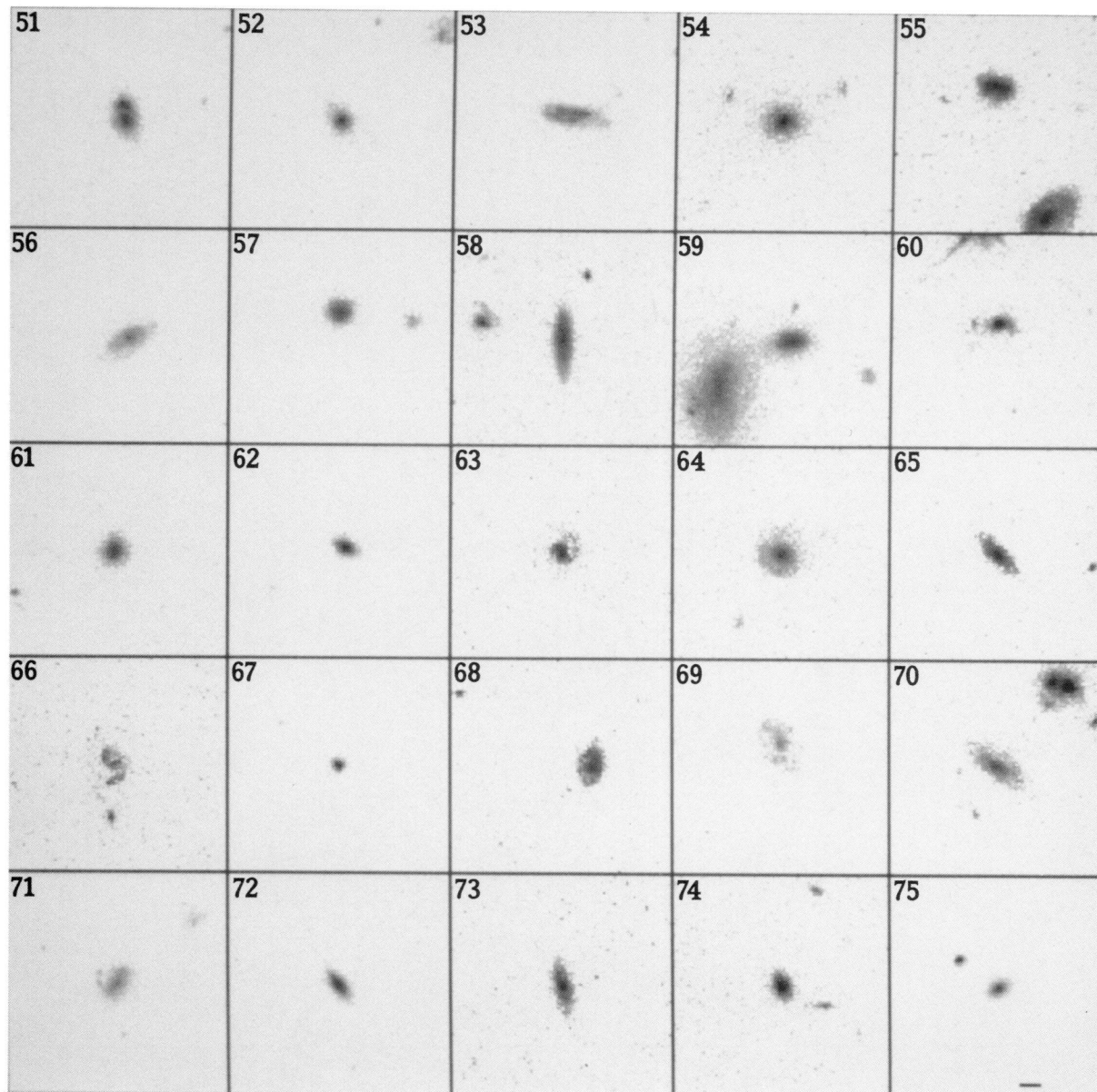


FIG. 1—Continued

FORBES et al. (see 437, L18)

TABLE 2
GALAXY PARAMETERS

Galaxy Number (1)	$V-I$ (2)	I (3)	Type (4)	Int.? (5)	Galaxy Number (1)	$V-I$ (2)	I (3)	Type (4)	Int.? (5)
1	0.92	16.54	E/S0	No	71	0.72	20.70	SBc	Yes
2	0.82	16.70	Sb	No	72	1.64	20.80	S0	No
3	0.92	16.74	E	No	73	1.42	20.80	Sb	No
4	1.06	17.20	E	No	74	1.80	20.80	S0	No
5	...	17.30	SBb	No	75	0.94	20.80	E/S0	Yes
6	0.96	18.05	S0p	No	76	1.56	20.80	Sa	No
7	...	18.10	SBb	Yes	77	1.13	20.80	Sb	No
8	1.05	18.50	E/S0	No	78	...	20.80	Sa	No
9	0.98	18.50	S0p	Yes	79	0.91	20.84	Sc	No
10	...	18.70	Sa	No	80	1.52	20.85	S0	No
11	0.76	18.70	Ep	Yes	81	1.24	20.85	Sb	No
12	1.27	18.84	Sb	No	82	1.00	20.90	b	No
13	1.10	18.85	Sd	No	83	1.08	20.90	i	No
14	0.83	18.90	Sb	Yes	84	0.99	20.90	d	No
15	1.02	18.90	Sa	No	85	...	20.90	E	No
16	0.83	18.90	Sb	No	86	...	20.90	d	Yes
17	1.59	19.00	Sb	No	87	0.96	20.90	S0	No
18	1.22	19.00	Sb	No	88	1.58	20.90	d	No
19	1.27	19.04	d	Yes	89	0.59	20.94	b	No
20	1.66	19.05	d	Yes	90	1.00	21.00	d	No
21	1.52	19.10	Ep	No	91	1.92	21.00	b	Yes
22	0.64	19.10	S0/a	No	92	1.81	21.00	Sa	No
23	0.66	19.15	Sc	Yes	93	...	21.00	d	No
24	1.11	19.20	E/S0p	Yes	94	1.72	21.00	Sa	No
25	1.01	19.20	Sc	No	95	0.84	21.04	b	No
26	0.73	19.40	d	Yes	96	1.64	21.04	Sa	No
27	1.04	19.50	Sc	No	97	1.41	21.10	d	No
28	0.98	19.60	Sb	Yes	98	0.87	21.10	i	No
29	1.43	19.60	Sb	No	99	0.77	21.10	SBc	No
30	0.83	19.60	Ep	Yes	100	2.13	21.10	i	No
31	0.88	19.74	SBb	No	101	1.10	21.10	b	No
32	0.87	19.75	Sc	No	102	...	21.10	i	No
33	1.04	19.75	Sb	No	103	...	21.10	Sc	No
34	1.18	19.75	dn	Yes	104	1.90	21.10	b	Yes
35	0.89	19.80	Sc	Yes	105	...	21.10	d	No
36	...	19.80	Sb	No	106	0.95	21.10	d	No
37	...	19.90	SBb	No	107	1.11	21.10	Sc	No
38	1.73	19.90	Sb	No	108	1.95	21.10	Sc	No
39	1.10	19.95	Sc	No	109	1.08	21.10	i	No
40	0.67	20.00	d	Yes	110	0.79	21.14	d	No
41	0.35	20.00	SBc	No	111	1.78	21.15	Irr	No
42	0.71	20.00	SBb	Yes	112	0.90	21.20	i	Yes
43	0.77	20.10	dn	Yes	113	1.20	21.20	b	No
44	1.41	20.10	Sb	No	114	0.69	21.20	d	Yes
45	0.71	20.14	Sb	No	115	...	21.20	dn	Yes
46	...	20.20	Ep	No	116	1.23	21.20	d	No
47	0.94	20.20	Sa	Yes	117	0.73	21.20	Sb	No
48	1.57	20.30	S0	Yes	118	1.42	21.24	d	No
49	2.18	20.30	i	No	119	...	21.25	d	No
50	1.02	20.30	Sb	No	120	1.41	21.30	Sb	No
51	1.23	20.35	dn	Yes	121	...	21.30	b	No
52	...	20.35	Sa	Yes	122	1.13	21.30	b	No
53	1.34	20.40	d	No	123	1.15	21.30	i	No
54	1.26	20.40	S0	No	124	...	21.30	d	No
55	0.94	20.40	i	Yes	125	...	21.30	d	Yes
56	0.79	20.50	Sc	No	126	0.76	21.30	d	No
57	...	20.50	E	No	127	1.42	21.30	i	No
58	0.81	20.55	Sc	No	128	1.75	21.30	d	Yes
59	0.71	20.60	i	Yes	129	1.05	21.35	i	No
60	0.70	20.60	Sb	No	130	1.19	21.40	d	No
61	...	20.60	S0	No	131	1.05	21.40	b	No
62	1.65	20.60	S0	No	132	1.15	21.40	d	Yes
63	1.56	20.60	SBa	No	133	1.76	21.40	d	Yes
64	1.56	20.65	i	Yes	134	1.68	21.40	i	Yes
65	1.38	20.65	Sb	No	135	0.55	21.40	b	Yes
66	0.26	20.70	i	Yes	136	0.91	21.40	d	Yes
67	1.27	20.70	i	Yes	137	1.70	21.50	b	No
68	1.16	20.70	Sc	No	138	1.24	21.50	E	No
69	...	20.70	Sc	Yes	139	0.86	21.50	i	Yes
70	1.41	20.70	Sa	No	140	1.43	21.50	d	No

TABLE 2—Continued

Galaxy Number (1)	$V-I$ (2)	I (3)	Type (4)	Int.? (5)	Galaxy Number (1)	$V-I$ (2)	I (3)	Type (4)	Int.? (5)
141	0.96	21.50	d	No	173	1.38	21.80	b	No
142	0.65	21.50	i	Yes	174	0.82	21.80	i	No
143	...	21.50	Sa	No	175	1.33	21.80	Sc	No
144	0.91	21.50	d	No	176	0.82	21.80	d	No
145	1.30	21.50	i	Yes	177	2.00	21.80	i	No
146	0.80	21.54	?	Yes	178	2.14	21.80	i	No
147	1.07	21.55	d	Yes	179	1.48	21.80	b	No
148	2.06	21.55	Sa	No	180	1.41	21.80	b	No
149	2.33	21.60	Sa	No	181	1.35	21.80	d	Yes
150	1.18	21.60	SBc	No	182	...	21.85	d	No
151	1.37	21.60	d	No	183	0.65	21.85	d	No
152	1.03	21.60	d	No	184	1.56	21.89	?	Yes
153	...	21.60	i	No	185	0.45	21.90	d	Yes
154	2.01	21.60	b	No	186	1.39	21.90	d	No
155	1.13	21.60	b	No	187	...	21.90	i	Yes
156	1.05	21.64	i	No	188	...	21.90	b	No
157	2.00	21.64	b	No	189	2.22	21.90	i	Yes
158	...	21.65	d	Yes	190	1.55	21.90	d	No
159	1.49	21.65	Sc	No	191	0.83	21.90	b	No
160	1.29	21.70	d	No	192	2.08	21.90	Sb	No
161	1.64	21.70	b	No	193	1.30	22.00	d	No
162	2.15	21.70	i	No	194	1.48	22.00	d	No
163	1.72	21.70	d	No	195	1.37	22.00	i	Yes
164	1.35	21.70	i	No	196	0.58	22.00	d	No
165	1.49	21.70	d	Yes	197	1.36	22.00	d	Yes
166	1.10	21.70	d	Yes	198	0.67	22.00	d	No
167	0.86	21.70	dn	Yes	199	1.07	22.00	d	Yes
168	1.38	21.70	b	No	200	1.19	22.00	d	No
169	0.85	21.70	b	No	201	0.63	22.00	d	No
170	...	21.75	d	Yes	202	2.01	22.00	d	Yes
171	1.95	21.75	S0	No	203	0.50	22.00	d	No
172	0.79	21.80	Irr	Yes					

Col. (1).—Galaxy ID. Col. (2).— $V_{606} - I_{814}$ color in a 0.3 radius aperture. Col. (3).—Total I_{814} magnitude. Col. (4).—Morphological type (b = bulge-dominated, i = intermediate, d = disk-dominated, dn = double nucleus. Col. (5).—Candidate for a ongoing merger or interaction.

59%. There is no significant difference in mix between fields with the most galaxies and those with the least. Taken at face value, the fractions quoted above imply no evidence for a decreased fraction of ellipticals with look-back time, contrary to what might be expected if spirals are frequently merging to form present-day ellipticals. However, such conclusions must be regarded as tentative, since a rigorous comparison with local field fractions requires modeling the luminosity function of each galaxy type subject to the limiting magnitude of the survey and any systematic biases present.

The observational evidence for a causal link between encounters and enhanced activity in a galaxy is quite strong. The activity can be in the form of a global starburst, but is often confined to the central kiloparsec (Keel et al. 1985). Theoretical work suggests that both interactions and mergers can deliver gas to the inner parts of a galaxy, providing fuel for a starburst or active galactic nucleus (see Barnes & Hernquist 1992). Thus the properties of the inner regions should be more sensitive to the effects of encounters than global measures. Our nuclear aperture (0.3) corresponds to $r = 1.2 h^{-1}$ kpc at $z = 0.5$ (for $h = H_0/100 \text{ km}^{-1} \text{ Mpc}^{-1}$, $q_0 = 0.05$). Before comparing merging/interacting galaxies with “normal” galaxies, we need to be sure that the two samples have a similar magnitude distribution and morphological mix, so as to avoid introducing any selection effects. We find that the magnitude distributions are almost identical; however, there is a small difference in the morphological mix (i.e., slightly more early-

type galaxies and fewer intermediate-type galaxies in the normal galaxy sample). In Figure 2 we show the nuclear colors for both the merging/interacting and normal galaxies (after correcting for the morphological mix). A Kolmogorov-Smirnov test indicates a less than 3% chance that the two distributions are taken from the same population. There is a weak tendency for the merging/interacting sample to have bluer nuclear colors, as might be expected if the encounter has led to increased star formation. If we look at the 50 galaxies with the bluest and the reddest centers, we find that 44% and 24%, respectively, are classified as merger/interacting. The statistical significance of this difference is $\sim 2 \sigma$.

6. CONCLUDING REMARKS

Using WFC-II images, we have defined a magnitude-limited sample of 203 field galaxies to $I \leq 22$, with an expected median redshift $z \sim 0.5$. For galaxies with $I < 21$, familiar Hubble types can be assigned. Our data will provide a useful comparison to WFC observations of cluster galaxies and thus facilitate study of the morphology-density relation at moderate redshift. Many galaxies in our sample appear peculiar, and often with nearby (projected) companions. We have correlated the colors in the central kiloparsec for these galaxies versus noninteracting galaxies for the first time at moderate redshifts. There is a weak trend (2σ) for interacting galaxies to have bluer nuclear colors.

Coordinates for the galaxies listed in Table 2 are available from D. A. F. in electronic form (forbes@lick.ucsc.edu).

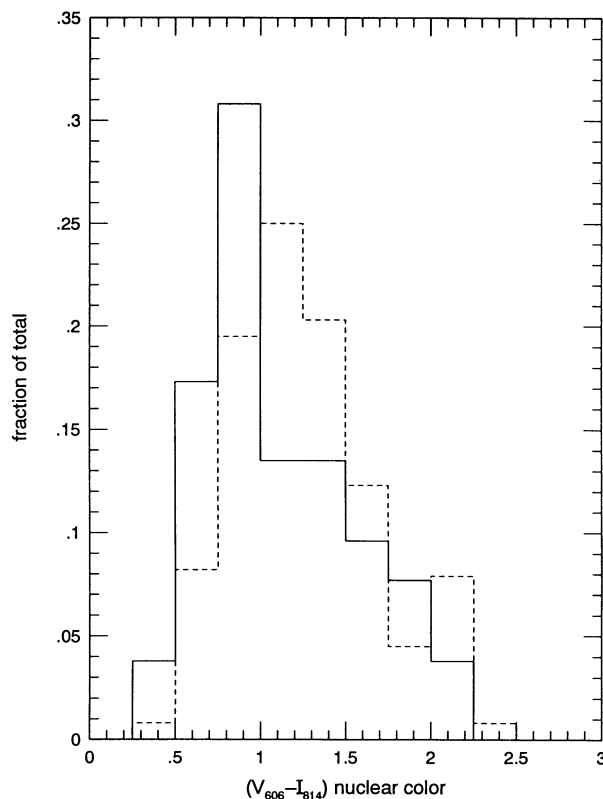


FIG. 2.—Histogram of the nuclear (central-kiloparsec) $V_{606} - I_{814}$ colors for the merging/interacting sample (solid lines) and the “normal” galaxies (dashed lines). There is a weak trend for the galaxies involved in an encounter to have a blue nucleus.

We thank E. Wyckoff, B. Santiago, M. Bershad, and the referee for help and useful discussions. P. McMillan of UCSC Media Services provided graphics support. We would also like

to thank the MDS team. The research was funded by *HST* grant GO-2684.04-87A.

REFERENCES

- Babul, A., & Rees, M. J. 1992, *MNRAS*, 255, 346
 Barnes, J. E., & Hernquist, L. 1992, *ARA&A*, 30, 705
 Broadhurst, T., Ellis, R. S., & Glazebrook, K. 1992, *Nature*, 355, 55
 Couch, W. J., Ellis, R. S., Sharples, R. M., & Smail, I. 1994, *ApJ*, 430, 121
 Dressler, A. 1980, *ApJ*, 236, 351
 Dressler, A., Oemler, A., Butcher, H. R., & Gunn, J. E. 1994, *ApJ*, 430, 107
 Frei, Z., & Gunn, J. E. 1994, *AJ*, 108, 1476
 Glazebrook, K., et al. 1994, in preparation
 Griffiths, R. E., et al. 1994a, *ApJ*, 435, L19
 ———. 1994b, *ApJ*, 437, 67
 Holtzman, J. A., et al. 1994, Initial Calibration of WFPC-II (Baltimore: STScI)
 Hubble, E., & Humason, M. L. 1931, *ApJ*, 74, 43
 Keel, W. C., Kennicutt, R. C., Hummel, E., & van der Hulst, J. M. 1985, *AJ*, 90, 708
 Lavery, R. J., Pierce, M. J., & McClure, R. D. 1992, *AJ*, 104, 2067
 Lilly, S. J. 1993, *ApJ*, 411, 501
 Phillips, A. C., et al. 1994a, *ApJ*, in press
 ———. 1994b, in preparation
 Postman, M., & Geller, M. J. 1984, *ApJ*, 281, 95
 Sandage, A. 1961, *The Hubble Atlas of Galaxies* (Washington, DC: Washington)
 Tresse, L., Hammer, F., Le Fevre, O., & Proust, D. 1993, *A&A*, 277, 53
 Whitmore, B. C., Gilmore, D. M., & Jones, C. 1993, *ApJ*, 407, 489